Published in final edited form as:

Eur Radiol. 2018 January ; 28(1): 133–142. doi:10.1007/s00330-017-4956-z.

Longitudinal Study of Sodium MRI of Articular Cartilage in Patients with Knee Osteoarthritis: Initial Experience with 16-Month Follow-Up

Guillaume Madelin, PhD[1,*], **Ding Xia, MSc**[1], **Ryan Brown, PhD**[1], **James Babb, PhD**[1], **Gregory Chang, MD**[1], **Svetlana Krasnokutsky, MD**[2], and **Ravinder R. Regatte, PhD**[1]

[1]New York University School of Medicine, Department of Radiology, 660 First Avenue, 4th Floor, New York, NY 10016, USA

[2]New York University School of Medicine, Department of Medicine, Rheumatology Division, 305 Second Avenue, New York, NY 10003, USA

Abstract

Objective—To evaluate the potential of sodium MRI to detect changes over time of apparent sodium concentration (ASC) in articular cartilage in patients with knee osteoarthritis (OA).

Materials and Methods—The cartilage of 12 patients with knee OA were scanned twice over a period of approximately 16 months with two sodium MRI sequences at 7 T: without fluid suppression (radial 3D), and with fluid suppression by adiabatic inversion recovery (IR). Changes between baseline and follow-up of mean and standard deviation of ASC (in mM), and their rate of change (in mM/day), were measured in the patellar, femorotibial medial, and lateral cartilage

---

[*]Corresponding author: New York University School of Medicine, Department of Radiology, Center for Biomedical Imaging, 660 First Avenue, 4th Floor, New York, NY 10016, USA, Tel: 212-263-3343, guillaume.madelin@nyumc.org.

Guarantor:
The scientific guarantor of this publication is Guillaume Madelin, PhD.

Conflict of interest:
The authors of this manuscript declare no relationships with any companies, whose products or services may be related to the subject matter of the article.

Statistics and biometry:
One of the authors has significant statistical expertise.

Compliance with ethical standards:
Informed consent:
Written informed consent was obtained from all subjects (patients) in this study.
Ethical approval:
Institutional Review Board approval was obtained.

Study subjects or cohorts overlap:
Some study subjects have been previously reported in Madelin G, et al. Articular cartilage: evaluation with fluid-suppressed 7.0-T sodium MR imaging in subjects with and subjects without osteoarthritis. Radiology. 2013;268(2):481-91. The present study is a follow-up study of the study published in Radiology.

Methodology:

- prospective
- longitudinal study/experimental
- performed at one institution

regions for each subject. A matched-pair Wilcoxon signed rank test was used to assess significance of the changes.

Results—Changes in mean and in standard deviation of ASC, and in their respective rate of change over time, were only statistically different when data was acquired with the fluid-suppressed sequence. A significant decrease (P=0.001) of approximately 70 mM in mean ASC was measured between the two IR scans.

Conclusion—Quantitative sodium MRI with fluid suppression by adiabatic IR at 7 T has the potential to detect a decrease of ASC over time in articular cartilage of patients with knee osteoarthritis.

Keywords

Osteoarthritis; Sodium; Magnetic Resonance Imaging; Cartilage; Glycosaminoglycans

INTRODUCTION

Osteoarthritis (OA) is a disease of the entire joint that can results from the breakdown of articular cartilage and underlying bone, but also from broken ligaments or meniscus[1; 2; 3]. It is the most common form of arthritis and a leading cause of chronic disability in the elderly population[4]. OA is generally considered to be a degenerative disease characterized mainly by an overall loss of glycosaminoglycan (GAG) in cartilage, along with disruption of the collagen fibres and disorganization of the collagen matrix, and a small increases in water content[5]. Generally, these early OA changes in GAG, collagen and water content precede the mechanical damage of cartilage and bone.

Many MRI methods[6] are being developed to provide quantitative information about the physiological changes in cartilage due to OA, such as: T2 mapping[7], T1ρ mapping[8], GAG chemical exchange saturation transfer (gagCEST)[9], delayed gadolinium enhanced MRI of cartilage (dGEMRIC)[10], diffusion tensor imaging (DTI)[11], and sodium MRI[12]. Sodium MRI[13] has been shown to strongly correlate with the GAG concentration in the cartilage[5; 14; 15; 16]. It is therefore a promising candidate imaging biomarker for monitoring loss of GAG and cartilage degradation over time in patients with OA, and also for monitoring the effects of disease-modifying OA drugs[17].

In a previous study[18], we demonstrated that quantitative sodium MRI with fluid suppression by inversion recovery with an adiabatic pulse at 7 T in cartilage could significantly differentiate asymptomatic subjects (controls) from patients with knee OA, as it is less sensitive to partial volume effects from surrounding synovial fluid than the acquisition without fluid suppression. In the present study, which is a follow-up to the previous one[18] and is based on the same patient cohort (twelve of the knee OA patients agreed to come back), we measured and compared the variations of apparent sodium concentration (ASC) in the articular cartilage with sodium MRI with and without fluid suppression by adiabatic inversion, at baseline and 16-month follow-up in patients with knee OA. The aim of this pilot study is to evaluate the potential of sodium MRI to detect changes over time of ASC in articular cartilage in patients with knee osteoarthritis (OA). The long-term goal of this work would be to assess GAG depletion in knee OA patients with longitudinal measurements of cartilage ASC using sodium MRI.

MATERIALS AND METHODS

Patients with OA

This study was approved by the institutional review board (IRB) and performed in compliance with Health Insurance Portability and Accountability Act (HIPAA). All subjects provided written informed consent. We scanned the knee cartilage of 12 patients with OA, selected from the NYU Hospital of Joint Diseases knee OA cohort[19]. Subject characteristics are provided in Table 1. These patients fulfilled the clinical OA symptoms defined by the American College of Rheumatology[20] (ACR) as well as radiographic evidence of tibial-femoral knee OA with Kellgren-Lawrence (KL) grade of 1–4 on the standardized weight-bearing fixed-flexion posterior-anterior knee radiographs at baseline[21]. The exclusion criteria were any inflammatory arthritis, prior traumatic knee injury or surgery on either knee, and history of bilateral knee replacements.

Hardware

All sodium images were acquired on a whole-body 7 T scanner (Siemens Healthcare, Erlangen, Germany) with a homemade double-tuned proton-sodium knee coil[22] (4-channel transmit-receive for proton, birdcage transmit and 8-channel receive for sodium).

Sodium MRI Acquisition

MRI sequences—Sodium images without fluid suppression were acquired using a ultrashort echo time (UTE) radial 3D sequence (R3D)[23]. Fluid suppression was obtained by inversion recovery (IR) using an adiabatic pulse and appropriate inversion time prior to the R3D sequence[24]. The adiabatic pulse was the WURST (Wideband Uniform Rate and Smooth Truncation) pulse[25] with a sweep range of 2 kHz and the sequence is referred to as IR WURST (IRW). The sequences were written in Sequence Tree 4.2.2[26] and compiled with the Siemens program IDEA VB15A/VB17A All sequence parameters, imaging gradients and RF pulses were exactly the same for the two scans. Images were reconstructed offline in Matlab (Mathworks, Natick, MA, USA) using a non-uniform fast Fourier transform (NUFFT) algorithm[27]. Details of the sequences and reconstruction parameters are presented in Table 2.

Acquisition protocol—All subjects were scanned at baseline and follow-up with both R3D and IRW sequences. A summary flowchart of the protocol for data acquisition and analysis is presented in Supplemental Figure S1. Data was acquired in the period 11/2011–06/2012 for baseline and in the period 02/2013–10/2013 for follow-up.

Image Post-Processing

Apparent sodium concentration maps—All sodium images were acquired in the presence of calibration phantoms made of 4% Agar gel with known sodium concentrations (100, 150, 200, 250 and 300 mM). After T1 and T2* correction of the phantom signal intensities ($T1 = 23$ ms, $T2^*_{short} = 2$ ms, $T2^*_{long} = 12$ ms), ASC maps were calculated using linear regression[18; 24], which was considered valid only when the coefficient of determination $R^2 \geq 0.99$, to improve robustness of the method against noise and phantom signal variations[28]. The ASC maps were then corrected for average T1 and T2* of cartilage *in vivo* (T1 = 20 ms, $T2^*_{short}$ = 1 ms, $T2^*_{long}$ = 13 ms) to increase accuracy of the quantification of sodium concentration in cartilage[29]. Since, on average, 25% of the volume in cartilage is made up of solids without any sodium, the final sodium maps were divided by a factor 0.75[18; 30; 31].

Image co-registration—For each subject, all four 3D datasets (R3D and IRW from baseline and follow-up) were co-registered using 3D Voxel Registration in Analyze 10.0 (AnalyzeDirect Inc., Overland Park, KS).

ASC measurements—Three regions-of-interest (ROI) of 40 pixels were drawn on the patellar (PAT), femoro-tibial lateral (LAT) and femoro-tibial medial (MED) cartilage, on 8 consecutives slices of the ASC maps using the following protocol for each subject: (1) For each consecutive slice, draw a large ROI surrounding the cartilage area where we want to make the measurement; (2) On the first R3D data (baseline), select 40 pixels with highest ASC values within the large ROI; (3) Generate a mask from this 40-pixel area; (4) Transpose this mask to all other three co-registered datasets (baseline IRW, follow-up R3D and follow-up IRW); (5) Measure the pixels values corresponding to the mask in each dataset; (6) Calculate the mean and standard deviation (std) of ASC over all 320 pixels (8 ROIs of 40 pixels). Examples of ROIs and masks to measure ASC values in PAT (transverse slice), MED and LAT (coronal slice) are shown in Figure 1. This procedure ensures that all the ASC values are measured at exactly the same locations in all 3D sodium datasets for each subject.

RF coil correction—A signal-to-noise ratio (SNR) map of the coil was calculated on a uniform cylindrical water phantom doped with 45 mM of NaCl that filled the coil volume[22], from a R3D acquisition with 15,000 projections and other parameters from Table 2. The SNR distribution was highest in the periphery and reduced toward the centre, which is typical of phased array coils (see Brown et al.[22] for the map), and therefore was used to correct the images from all subjects prior to ASC quantification[18].

Statistical Analysis

For each subject the change in each measure (mean or std of ASC, in mM) from each region as determined by each sequence was computed as the value at baseline minus the value at follow-up. As a result, positive change corresponds to a decline in value over time. The regional rate of change in each measure was computed for each subject as the change divided by the time between scans for that subject. Rates of change are expressed in units of mM/day. For each measure within each region the matched-pair Wilcoxon signed rank test was used to assess whether the measure changed over time and to compare sequences in terms of the change over time and the rate of change. Exact Mann-Whitney tests were used to compare males and females in terms of the change and rate of change in each regional measure. Spearman rank correlations were used to assess the relationship of the change and rate of change in each regional measure with age, weight and KL score. Statistical significance is defined as P value <0.05. All statistical tests were conducted at the two-sided 5% significance level using SAS 9.3 (SAS Institute, Cary, NC).

RESULTS

Sodium Concentration Maps

Figure 2 shows representative transverse and coronal ASC maps through the knee cartilage from the same OA patient (KL=1) at baseline (scan 1) and follow-up (scan 2, mean delay = 478 days ~ 16 months later), calculated from radial 3D (R3D, no fluid suppression) and IR WURST (IRW, fluid suppression) acquisitions. The ASC measured with R3D look very similar in both scans, while a greater difference in ASC can be visually detected with IRW in all three cartilage regions.

Figure 3 shows the distributions of the ASC values measured in all voxels of all the ROIs of all subjects, from R3D and IRW acquisitions, for individual cartilage compartments (PAT, MED, LAT). We can visually detect a slight overall shift to the left (lower ASC) between scan 1 and 2 for the R3D measurements, while this shift is noticeably larger for the IRW measurements.

Figure 4 shows box plots of mean and std of ASC measured in PAT, MED and LAT compartments and calculated from R3D and IRW acquisitions, for all OA patients, at baseline (scan 1) and follow-up (scan 2). All ASC measures (mean and std) in all compartments show a statistically significant decrease between baseline and follow-up when calculated from IRW acquisitions. When data is acquired using R3D, only the mean ASC in LAT compartment shows a significant decrease. See Table 3 for statistics.

Figure 5 shows scatter plots of mean and std of ASC measured in PAT, MED and LAT compartments, and calculated from R3D and IRW acquisitions, for all OA patients: baseline (scan 1) vs. follow-up (scan 2). We can notice that for R3D, all data points are close to the diagonal (no change in measurement), while for IRW most of the data points are below the diagonal (decrease in measurement).

Statistical Analysis

The time between scans of each patient had a mean ± std of 477.67 ± 33.3 days (min-max range = 417–582 days) with a coefficient of variation (CV) of 8.0%. This small CV implies that results based on change and rate of change of ASC will be highly consistent in terms of correlations and P values.

Table 3 presents the mean, std, median and inter-quartile range (IQR) of the within subject change in each measure of ASC in mM, and the rate of change in each measure of ASC in mM/day, within each cartilage region as determined using each sequence. Each P value is calculated test to assess whether the measure changed over time, or whether the rate of change in the measure differed from zero. All changes of mean and std of ASC, and rates of change of mean and std of ASC, over the follow-up delay, were statistically significant for all cartilage compartments when measured using IRW. R3D data shows a significant decrease only for the mean ASC and for the rate of change in mean ASC in the patellar cartilage. For IRW, decrease in mean ASC was in the range 67.5–73.3 mM, and decrease in std of ASC was in the range 9.6–14.8 mM, in whole cartilage. For R3D, the decrease in mean ASC was much smaller (less than half of IRW), in the range 7.2–31.4 mM, and the decrease in std of ASC was also very small compared to IRW, in the range 0.8–3.6 mM. Rates of changes for IRW were in the range 0.139–0.149 mM/day for mean ASC, and 0.020–0.030 mM/day for std of ASC. Rates of changes in mean and std of ASC from R3D were also much smaller than from IRW, in the range 0.014–0.064 mM/day and 0.002–0.007 mM/day, respectively.

Complementary results from the statistical analysis are shown in Tables S1, S2, S3 and S4 of the Supplemental Material. Table S1 presents the mean, std, median and IQR of the within subject difference between sequences (IRW minus R3D) in terms of the change in each measure of ASC in mM, and in terms of the rate of change in each measure of ASC in mM/day, within each cartilage region. In all cases the sequences differed significantly for change of mean and std of ASC, and for rate of change of mean and std of ASC over time, for each subject. Table S2 presents the mean, std, median and IQR of the within subject change in each measure of ASC within each cartilage region as determined using each sequence for each gender. No significant difference was detected between measurements in male and female, except for the measure of std of ASC from R3D in PAT. Table S3 presents the mean, std, median and IQR of the within subject rate of change in each measure of ASC within each cartilage region as determined using each sequence for each gender. No significant difference was detected between measurements in male and female, except for the measure of std of ASC from R3D in PAT. Table S4 presents the Spearman correlation (R) and P value for the association of the change and rate of change in each regional measure of ASC with age, weight and KL grade. No correlation was found significant between age and any change or rate of change in the measures of mean and std of ASC. A significant correlation was found between KL grade and change in mean ASC in LAT (R=0.69, P=0.013), and between KL grade and change in std of ASC in MED (R=0.79, P=0.002), for IRW acquisition only. Similar correlations between KL grades and the rates of change in measures of ASC in the same cartilage regions were noticed for IRW data. A significant correlation was found between weight and change in mean ASC (R=0.65, P=0.023), in PAT for R3D acquisition. Significant correlation were noticed between weight and the rate of change in mean ASC in PAT from R3D (R=0.64,P=0.025), the rate of change in std of ASC in PAT from R3D (R=0.61,P=0.037), and the rate of change in std of ASC in MED from IRW (R=0.58, P=0.046).

DISCUSSION

From the results presented in Table 3, we can assert that measurements of the changes in mean ASC and in std of ASC, and in their respective rate of change over time, were only statistically different between baseline and follow-up when data was acquired with the fluid-suppressed sequence IRW. Moreover, for each subject, the difference in all results from IRW and R3D was significantly different, with the changes measured from IRW data much larger (by at least a factor 2) than the changes measured from R3D data. This is mainly due to a reduction of partial volume effect of the surrounding synovial fluid ([Na^+] ~140 mM) by inversion recovery.

Acquiring sodium data with MRI is challenging due to the fact that the sodium MR signal in cartilage is about 3,500 times lower than the proton signal, and exhibits very fast relaxation that necessitates specific UTE acquisition sequences such as radial 3D[13]. Due to these challenges, sodium MRI is generally acquired with low resolution (3.3 mm isotropic in our case, which is similar to the thickness of human knee cartilage[32]) and long acquisition times (16 min for R3D and 23 min for IRW) at 7 T. We showed that IRW reduces partial volume effects of surrounding fluids associated with the coarse resolution. Going forward, this method could be implemented with more efficient UTE 3D sequences such as FLORET[33] or TPI[34] which can increase signal-to-noise efficiency by 40–50%, and exploit data undersampling and compressed sensing (CS) reconstruction[35; 36]. The combination of ultra-high field (7 T) with fast 3D acquisition with fluid suppression and optimized multi-channel CS reconstruction could allow to acquire ASC maps with higher resolution (about 2 mm) within 10 min. On the other hand, we can notice that the better performance of IRW over R3D is valid only for voxels containing cartilage and synovial fluid. For thin structures such as femoral cartilage, it might be more advantageous to trade the higher signal intensity of R3D for even higher spatial resolution (1 mm) with reduced partial volume effect from synovial fluid and other surrounding tissues.

Although the sample size was small (12 subjects), we were still able to detect longitudinal reductions in cartilage apparent sodium content, which provides support for the potential use of sodium MRI to monitor disease progression in osteoarthritis. Unfortunately, progression of OA could not be assessed on these patients, and KL grades at follow-up were therefore not available for comparison with baseline and for possible correlation between KL grade evolution and sodium quantification in patients. We could not confirm clinically that the level of OA progressed during follow-up. In the future, larger longitudinal studies are needed with early OA subjects, along with healthy controls, to prove that longitudinal reductions in sodium (or GAG) content can be detected with sodium IRW MRI, and have correlations with the later development of joint space narrowing on radiographs and the evolution of KL grade over time.

One limitation of this study is the lack of follow-up scans on control subjects, which could be a good indicator of the accuracy of the proposed method to detect changes in ASC in cartilage due to OA compared to normal aging. It can however be noticed that a CV of 8–10% can be expected for ASC quantification from IRW[37]. In this study, we measured a decrease of ASC of ~70 mM from baseline in the range 200–250 mM, corresponding to a variation of 28–35%. We can thus assume that this decrease is probably not due to acquisition uncertainties.

Another limitation is that, due to the small sample size, no conclusive relationship between KL grade, weight and ASC measures can be made. No significant statistical difference was found between male and female results and no correlation was found between age and the measurements of mean and std of ASC.

A final limitation is that the sodium T1 and T2* relaxation times in cartilage were considered fixed in the quantification algorithm, as measured from healthy subjects in a prior study[29]. However, these relaxation times can change during cartilage degradation[38], due to GAG depletion and collagen matrix deterioration, and influence ASC quantification. Measuring relaxation times in vivo can be very time consuming[29], but would bring new fundamental information about cartilage degradation. An estimation of the error propagation[24; 28; 39] of variations of T1, $T2_{short}$ and $T2_{long}$ of cartilage (from baseline values of 20 ms, 1 ms and 13 ms respectively[29]) of 10% each leads to a total uncertainty of 9% in mean ASC, and variations of 20% in relaxation times lead to an uncertainty of 19% in mean ASC for IRW. When no inversion is involved (R3D), the uncertainty is <1% in all cases. It is therefore difficult in the present study to assign which part of the loss of ASC is due to real loss of sodium content within the cartilage or due to variations of relaxation times, but it can be noticed that both are expected to be related to loss of GAG (and also collagen matrix degradation for the relaxation part) and general cartilage degradation. We will therefore keep in mind that the ASC measured with the present IRW protocol represent only an "apparent" sodium concentration that is also influenced by changes in relaxation times. Once a fast method of sodium data acquisition based on high field, efficient sequence and CS reconstruction is implemented, T1 and T2* measurement could potentially be added to the scanning protocol and help separate the effects of relaxation times on the ASC measured, along with complementary proton MRI[6].

In conclusion, this study shows that quantitative sodium MRI with fluid suppression by adiabatic inversion can detect changes in ASC over time in the articular cartilage of patients with knee osteoarthritis.

Supplementary Material

Refer to Web version on PubMed Central for supplementary material.

Acknowledgments

Funding:

This study has received funding by National Institutes of Health (grant nos. 1R01AR067156, 1R01AR060238, 1R01AR056260, 1R01AR068966, 1R03AR065763, 1R01NS097494, 1P41EB017183).

ABBREVIATIONS AND ACRONYMS

^{1}H	Proton
^{23}Na	Sodium
ASC	Apparent Sodium Concentration
GAG	Glycosaminoglycan
IR	Inversion Recovery
IRW	IR WURST
KL	Kellgren-Lawrence
LAT	Femoro-tibial Lateral cartilage

MED	Femoro-tibial Medial cartilage
MRI	Magnetic resonance Imaging
OA	Osteoarthritis
PAT	Patellar cartilage
R3D	Radial 3D
UTE	Ultrashort Echo Time
WURST	Wideband Uniform Rate and Smooth Truncation

References

1. Sharma L. Osteoarthritis year in review 2015: clinical. Osteoarthritis Cartilage. 2016; 24:36–48. [PubMed: 26707991]
2. Glyn-Jones S, Palmer AJ, Agricola R, Price AJ, Vincent TL, Weinans H, Carr AJ. Osteoarthritis. Lancet. 2015; 386:376–87. [PubMed: 25748615]
3. Alizai H, Roemer FW, Hayashi D, Crema MD, Felson DT, Guermazi A. An update on risk factors for cartilage loss in knee osteoarthritis assessed using MRI-based semiquantitative grading methods. Eur Radiol. 2015; 25:883–93. [PubMed: 25377771]
4. Lawrence RC, Felson DT, Helmick CG, Arnold LM, Choi H, Deyo RA, Gabriel S, Hirsch R, Hochberg MC, Hunder GG, Jordan JM, Katz JN, Kremers HM, Wolfe F. Estimates of the prevalence of arthritis and other rheumatic conditions in the United States. Part II. Arthritis Rheum. 2008; 58:26–35. [PubMed: 18163497]
5. Borthakur A, Mellon E, Niyogi S, Witschey W, Kneeland JB, Reddy R. Sodium and T1rho MRI for molecular and diagnostic imaging of articular cartilage. NMR Biomed. 2006; 19:781–821. [PubMed: 17075961]
6. Braun HJ, Gold GE. Diagnosis of osteoarthritis: imaging. Bone. 2012; 51:278–88. [PubMed: 22155587]
7. Smith HE, Mosher TJ, Dardzinski BJ, Collins BG, Collins CM, Yang QX, Schmithorst VJ, Smith MB. Spatial variation in cartilage T2 of the knee. J Magn Reson Imaging. 2001; 14:50–5. [PubMed: 11436214]
8. Regatte RR, Akella SV, Borthakur A, Kneeland JB, Reddy R. In vivo proton MR three-dimensional T1rho mapping of human articular cartilage: initial experience. Radiology. 2003; 229:269–74. [PubMed: 14519880]
9. Ling W, Regatte RR, Navon G, Jerschow A. Assessment of glycosaminoglycan concentration in vivo by chemical exchange-dependent saturation transfer (gagCEST). Proc Natl Acad Sci U S A. 2008; 105:2266–70. [PubMed: 18268341]
10. Bashir A, Gray ML, Burstein D. Gd-DTPA2- as a measure of cartilage degradation. Magn Reson Med. 1996; 36:665–73. [PubMed: 8916016]
11. Filidoro L, Dietrich O, Weber J, Rauch E, Oerther T, Wick M, Reiser MF, Glaser C. High-resolution diffusion tensor imaging of human patellar cartilage: feasibility and preliminary findings. Magn Reson Med. 2005; 53:993–8. [PubMed: 15844163]
12. Reddy R, Insko EK, Noyszewski EA, Dandora R, Kneeland JB, Leigh JS. Sodium MRI of human articular cartilage in vivo. Magn Reson Med. 1998; 39:697–701. [PubMed: 9581599]
13. Madelin G, Regatte RR. Biomedical applications of sodium MRI in vivo. J Magn Reson Imaging. 2013; 38:511–29. [PubMed: 23722972]
14. Lesperance LM, Gray ML, Burstein D. Determination of fixed charge density in cartilage using nuclear magnetic resonance. J Orthop Res. 1992; 10:1–13. [PubMed: 1309384]

15. Shapiro EM, Borthakur A, Dandora R, Kriss A, Leigh JS, Reddy R. Sodium visibility and quantitation in intact bovine articular cartilage using high field (23) Na MRI and MRS. J Magn Reson. 2000; 142:24–31. [PubMed: 10617432]
16. Shapiro EM, Borthakur A, Gougoutas A, Reddy R. 23Na MRI accurately measures fixed charge density in articular cartilage. Magn Reson Med. 2002; 47:284–91. [PubMed: 11810671]
17. Qvist P, Bay-Jensen AC, Christiansen C, Dam EB, Pastoureau P, Karsdal MA. The disease modifying osteoarthritis drug (DMOAD): Is it in the horizon? Pharmacol Res. 2008; 58:1–7. [PubMed: 18590824]
18. Madelin G, Babb J, Xia D, Chang G, Krasnokutsky S, Abramson SB, Jerschow A, Regatte RR. Articular cartilage: evaluation with fluid-suppressed 7.0-T sodium MR imaging in subjects with and subjects without osteoarthritis. Radiology. 2013; 268:481–91. [PubMed: 23468572]
19. Attur M, Wang HY, Kraus VB, Bukowski JF, Aziz N, Krasnokutsky S, Samuels J, Greenberg J, McDaniel G, Abramson SB, Kornman KS. Radiographic severity of knee osteoarthritis is conditional on interleukin 1 receptor antagonist gene variations. Ann Rheum Dis. 2010; 69:856–61. [PubMed: 19934104]
20. Altman R, Asch E, Bloch D, Bole G, Borenstein D, Brandt K, Christy W, Cooke TD, Greenwald R, Hochberg M, et al. Development of criteria for the classification and reporting of osteoarthritis. Classification of osteoarthritis of the knee. Diagnostic and Therapeutic Criteria Committee of the American Rheumatism Association. Arthritis Rheum. 1986; 29:1039–49. [PubMed: 3741515]
21. Kellgren JH, Lawrence JS. Radiological assessment of osteo-arthrosis. Ann Rheum Dis. 1957; 16:494–502. [PubMed: 13498604]
22. Brown R, Madelin G, Lattanzi R, Chang G, Regatte RR, Sodickson DK, Wiggins GC. Design of a nested eight-channel sodium and four-channel proton coil for 7T knee imaging. Magn Reson Med. 2012 (in print).
23. Nielles-Vallespin S, Weber MA, Bock M, Bongers A, Speier P, Combs SE, Wohrle J, Lehmann-Horn F, Essig M, Schad LR. 3D radial projection technique with ultrashort echo times for sodium MRI: clinical applications in human brain and skeletal muscle. Magn Reson Med. 2007; 57:74–81. [PubMed: 17191248]
24. Madelin G, Lee JS, Inati S, Jerschow A, Regatte RR. Sodium inversion recovery MRI of the knee joint in vivo at 7T. J Magn Reson. 2010; 207:42–52. [PubMed: 20813569]
25. Kupce E, Freeman R. Adiabatic pulses for wide-band inversion and broadband pulse. J Magn Reson A. 1995; 115:273–276.
26. Magland J, Wehrli FW. ISMRM, Seattle, WA, USA. 2006
27. Greengard L, Lee JY. Accelerating the nonuniform fast Fourier transform. Siam Review. 2004; 46:443–454.
28. Madelin G, Kline R, Walvick R, Regatte RR. A method for estimating intracellular sodium concentration and extracellular volume fraction in brain in vivo using sodium magnetic resonance imaging. Sci Rep. 2014; 4:4763. [PubMed: 24755879]
29. Madelin G, Jerschow A, Regatte RR. Sodium relaxation times in the knee joint in vivo at 7T. NMR Biomed. 2012; 25:530–7. [PubMed: 21853493]
30. Borthakur A, Shapiro EM, Akella SV, Gougoutas A, Kneeland JB, Reddy R. Quantifying sodium in the human wrist in vivo by using MR imaging. Radiology. 2002; 224:598–602. [PubMed: 12147862]
31. Wheaton AJ, Borthakur A, Shapiro EM, Regatte RR, Akella SV, Kneeland JB, Reddy R. Proteoglycan loss in human knee cartilage: quantitation with sodium MR imaging--feasibility study. Radiology. 2004; 231:900–5. [PubMed: 15163825]
32. Shepherd DE, Seedhom BB. Thickness of human articular cartilage in joints of the lower limb. Ann Rheum Dis. 1999; 58:27–34. [PubMed: 10343537]
33. Pipe JG, Zwart NR, Aboussouan EA, Robison RK, Devaraj A, Johnson KO. A new design and rationale for 3D orthogonally oversampled k-space trajectories. Magn Reson Med. 2011; 66:1303–11. [PubMed: 21469190]
34. Boada FE, Gillen JS, Shen GX, Chang SY, Thulborn KR. Fast three dimensional sodium imaging. Magn Reson Med. 1997; 37:706–15. [PubMed: 9126944]

35. Lustig M, Donoho D, Pauly JM. Sparse MRI: The application of compressed sensing for rapid MR imaging. Magn Reson Med. 2007; 58:1182–95. [PubMed: 17969013]

36. Madelin G, Chang G, Otazo R, Jerschow A, Regatte RR. Compressed sensing sodium MRI of cartilage at 7T: preliminary study. J Magn Reson. 2012; 214:360–5. [PubMed: 22204825]

37. Madelin G, Babb JS, Xia D, Chang G, Jerschow A, Regatte RR. Reproducibility and repeatability of quantitative sodium magnetic resonance imaging in vivo in articular cartilage at 3 T and 7 T. Magn Reson Med. 2012; 68:841–9. [PubMed: 22180051]

38. Insko EK, Kaufman JH, Leigh JS, Reddy R. Sodium NMR evaluation of articular cartilage degradation. Magn Reson Med. 1999; 41:30–4. [PubMed: 10025608]

39. Ku H. Notes on the use of propagation of error formulas. Journal of Research of the National Bureau of Standards. 1966; 70

KEY POINTS

- Sodium MRI can detect apparent sodium concentration (ASC) in cartilage
- Longitudinal study: sodium MRI can detect changes in ASC over time
- Potential for follow-up studies of cartilage degradation in knee osteoarthritis

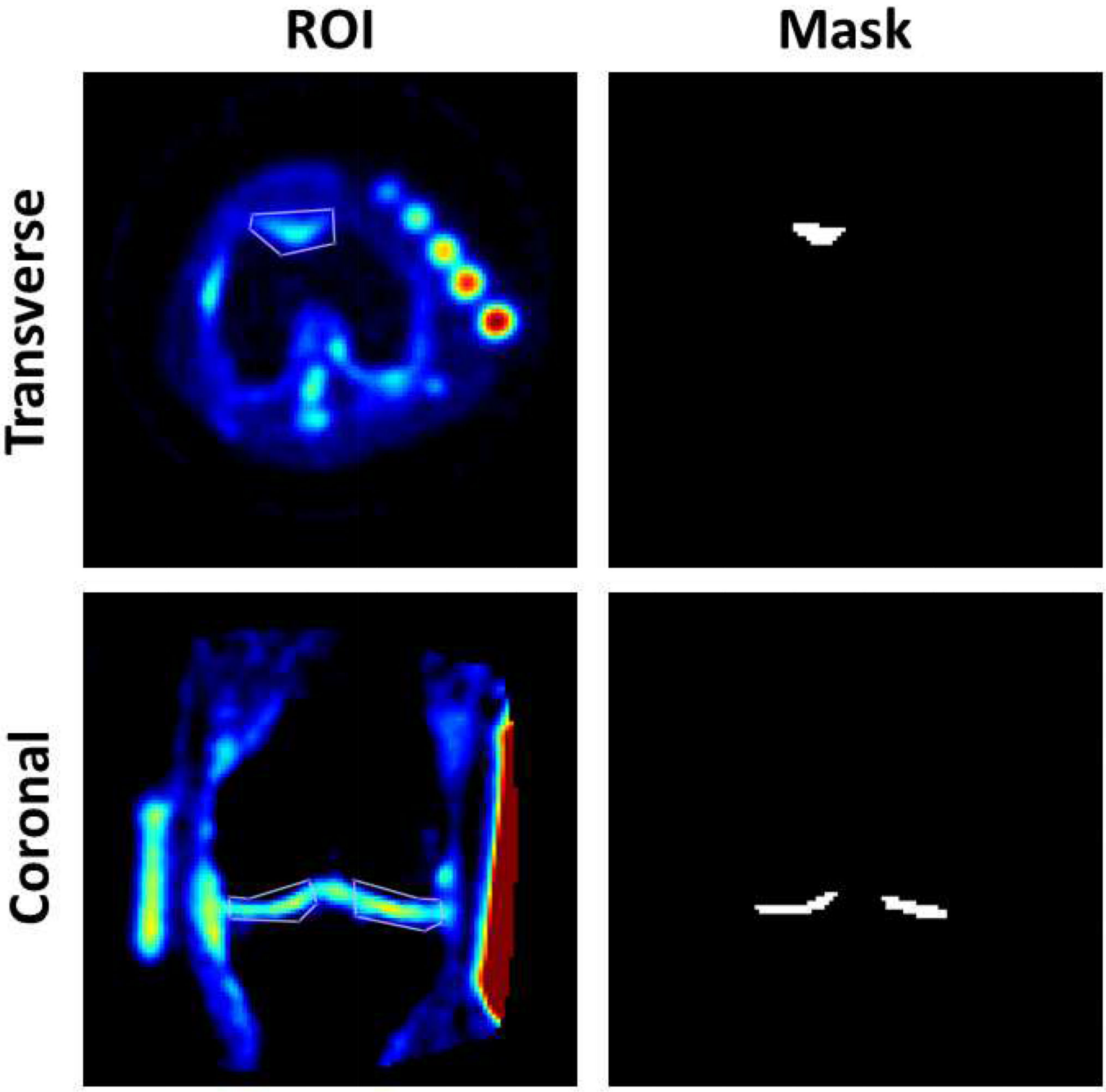

Figure 1.

Examples of large regions-of-interest (ROIs) and masks generated from 40 pixels with the highest values within the large ROIs, on a transverse slice showing patellar cartilage (PAT), and on a coronal slice showing femorotibial lateral (LAT) and medial (MED) cartilage. These large ROIs and masks are generated on the first dataset acquired on each subject (R3D at baseline). These masks are then transposed to the three other co-registered datasets (baseline R3D, follow-up R3D, follow-up IRW) where all 40 corresponding pixel values are measured. This procedure ensures that all the ASC values are measured at exactly the same locations in all 3D sodium datasets for each subject.

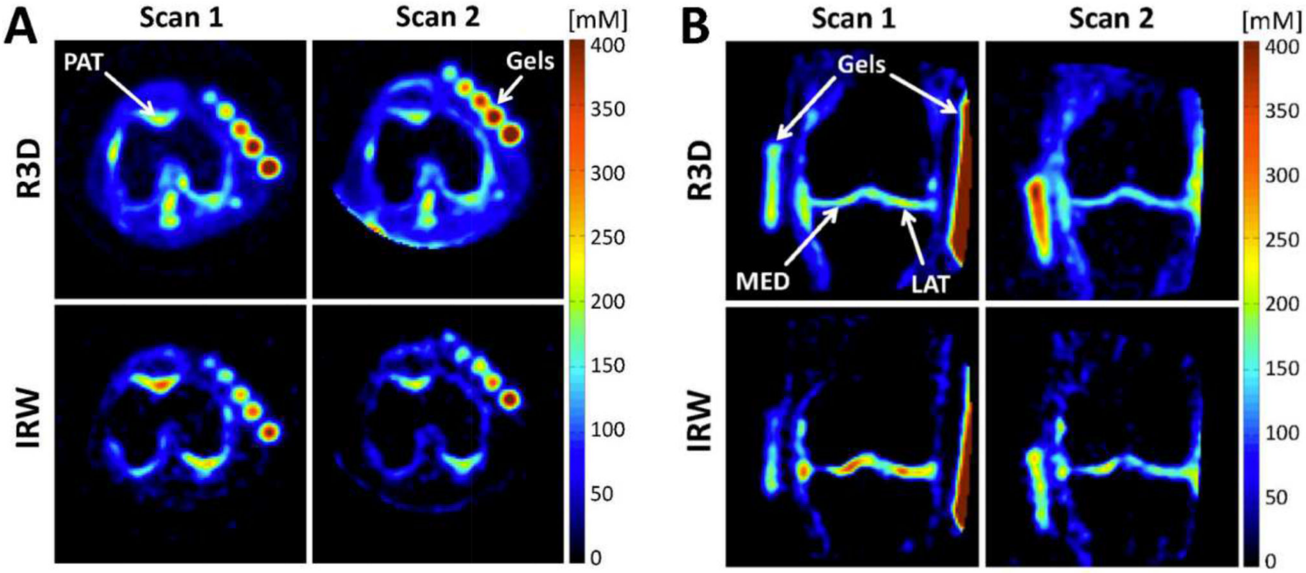

Figure 2.

Sodium maps from one OA patient, reconstructed from data acquired with fluid suppression (sequence IRW) and without fluid suppression (sequence R3D), at baseline (scan 1) and 16-month follow-up (scan 2). **A.** Transverse slices showing patellar cartilage (PAT). **B.** Coronal slices showing femorotibial lateral (LAT) and medial (MED) cartilage. The apparent sodium concentrations (ASC) measured with R3D look very similar in both scans, while a higher difference of ASC can be detected visually with IRW in PAT, MED and LAT.

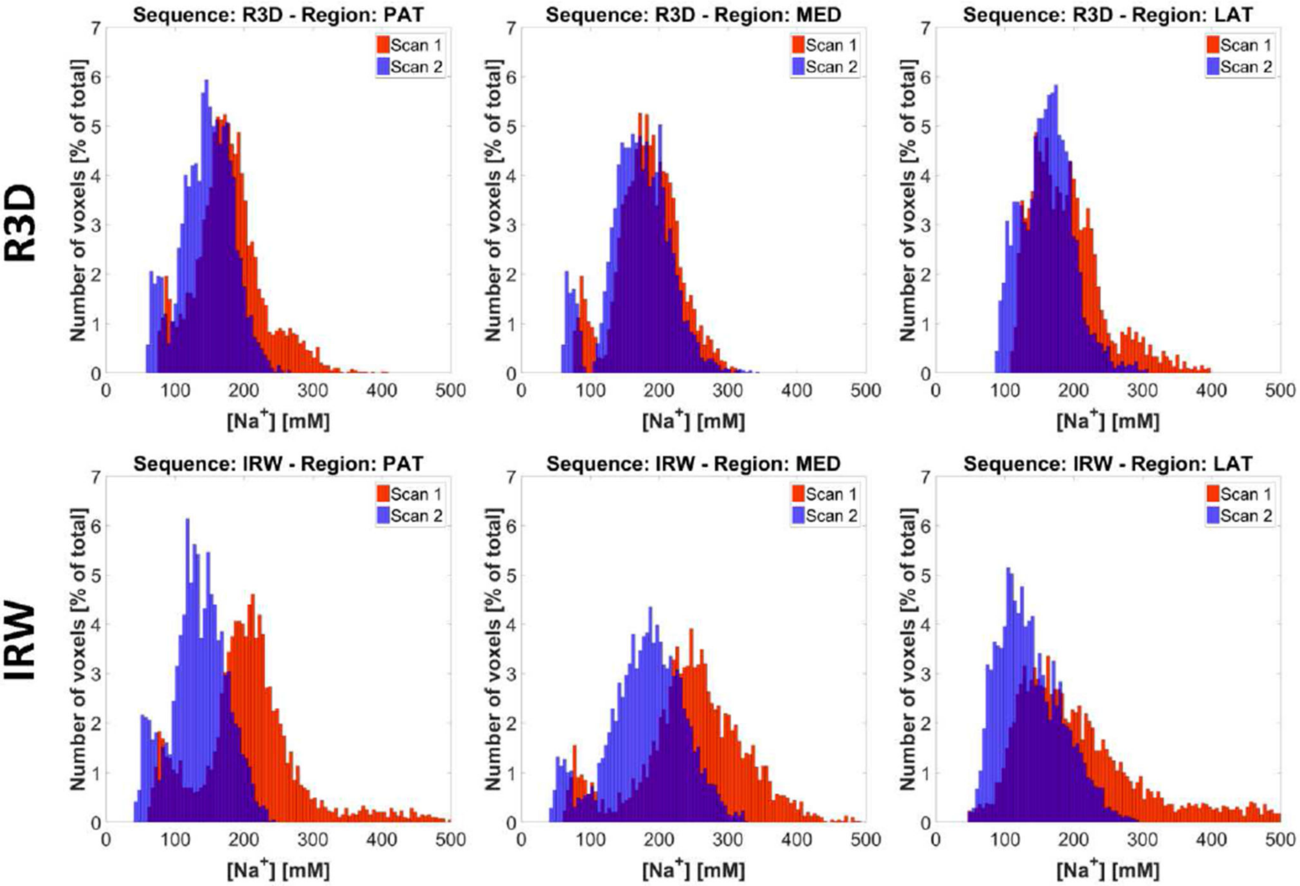

Figure 3.

Distribution (histograms) of the apparent sodium concentrations (ASC) measured in all voxels of all the ROIs of all subjects, from R3D acquisition (no fluid suppression) and from IRW acquisition (fluid suppression), for individual cartilage compartments (PAT, MED, LAT).

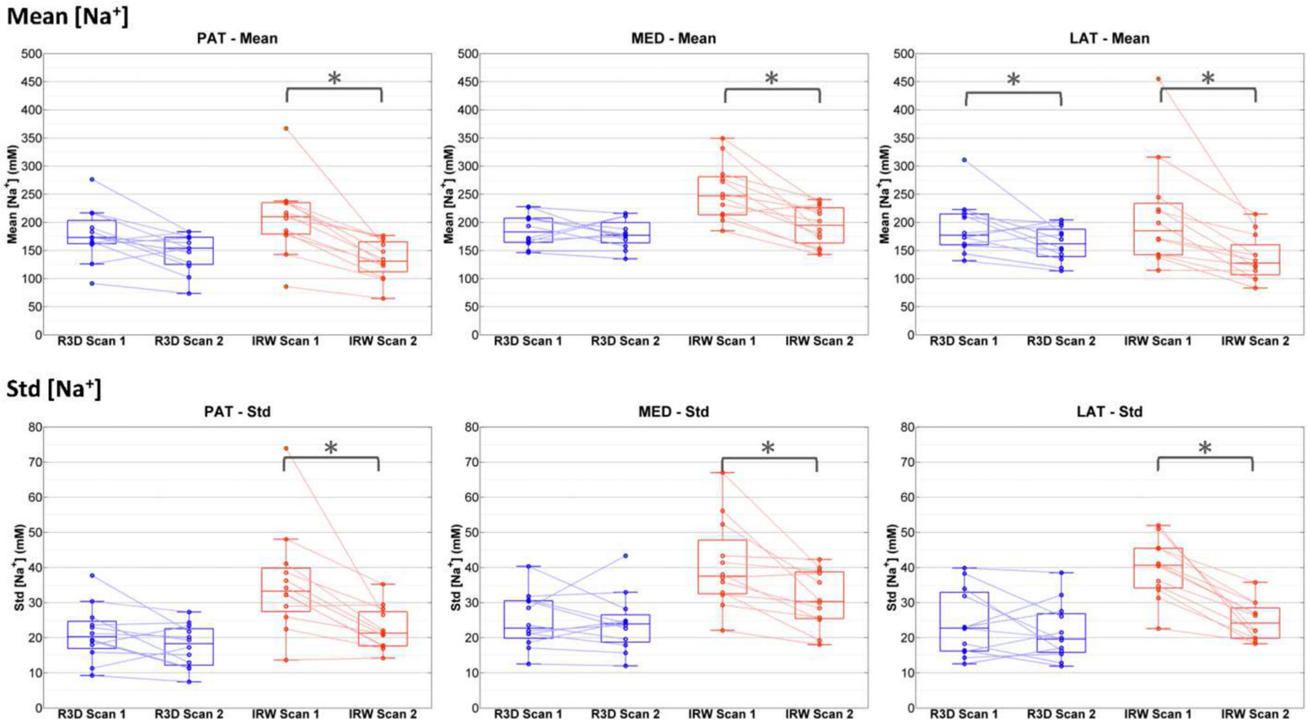

Figure 4.

Box plots of mean and standard deviation (std) of apparent sodium concentration (ASC) measured in PAT, MED and LAT cartilage compartments and calculated from R3D (blue) and IRW (red) acquisitions, for all 12 OA patients, at baseline (scan 1) and 16-month follow-up (scan 2). The star (*) represents statistical significance (P<0.05).

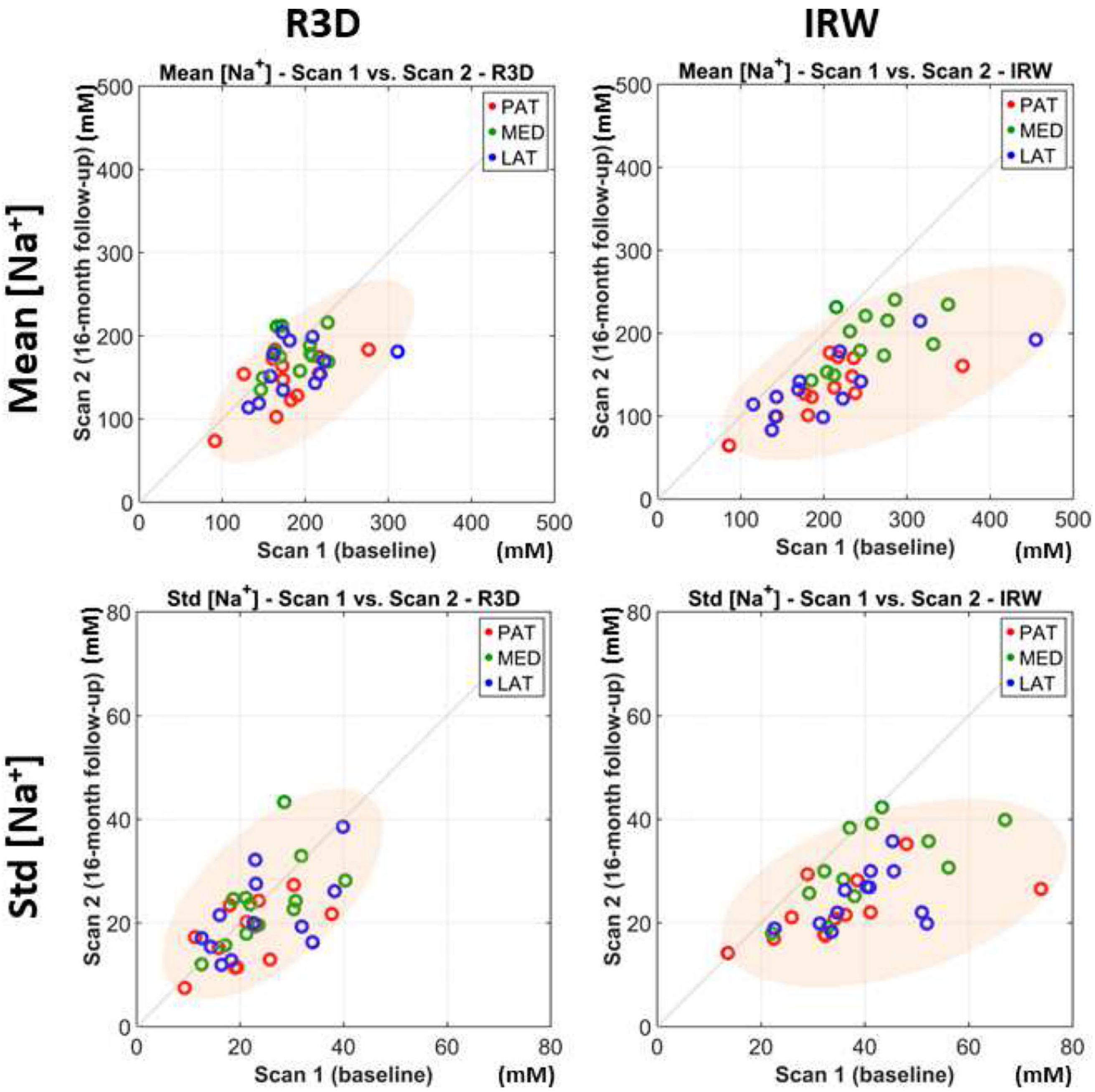

Figure 5.

Scatter plots of mean and standard deviation (std) of apparent sodium concentration (ASC) measured in PAT, MED and LAT cartilage compartments, and calculated from R3D (blue) and IRW (red) acquisitions, for all 12 OA patients: baseline (scan 1) vs. 16-month follow-up (scan 2).

Table 1

Knee OA patients characteristics at baseline.

		Kellgren-Lawrence (KL) Grade				
Subjects	**Characteristics**	**All**	**1**	**2**	**3**	**4**
All	Number	12	7	3	2	0
	Mean age (y)	65.8 ± 11.4	69.7 ± 12.4	57.7 ± 7.2	71.5 ± 6.4	0
	Age range (y)	47–81	47–81	53–66	67–76	0
	Mean weight (kg)	75.1 ± 10.9	73.7 ± 13.1	79.3 ± 9.1	73.5 ± 6.4	0
	Weight range (kg)	58–93	58–93	69–86	69–78	0
Men	Number	4	2	1	1	0
	Mean age (y)	69.3 ± 11.1	74.0 ± 4.2	53.0 ± 0.0	76.0 ± 0.0	0
	Age range (y)	53–76	71–77	53	76	0
	Mean weight (kg)	83.0 ± 8.1	84.0 ± 12.7	86.0 ± 0.0	78.0 ± 0.0	0
	Weight range (kg)	75–93	75–93	86	78	0
Women	Number	8	5	2	1	0
	Mean age (y)	66.0 ± 10.3	68.2 ± 13.3	60.0 ± 8.5	67.0 ± 0.0	0
	Age range (y)	47–81	47–81	53–66	67	0
	Mean weight (kg)	71.1 ± 10.3	69.6 ± 12.0	76.0 ± 9.9	69.0 ± 0.0	0
	Weight range (kg)	58–85	58–85	69–83	69	0

Table 2

Sodium acquisition sequence and reconstruction parameters

Parameters	Unit	Radial 3D (R3D)	IR WURST (IRW)
Number of Radial Projections	-	10,000	10,000
Repetition Time (TR)	ms	100	140
Echo Time (TE)	ms	0.4	0.4
Flip Angle (FA)	degree	90	90
Isotropic Field of View (FOV)	mm	200	200
Dwell Time	μs	80	80
Adiabatic Inversion Pulse Amplitude	Hz	-	240
Adiabatic Inversion Pulse Length	ms	-	10
Inversion Time (TI)	ms	-	24
Nominal Resolution [*]	mm	2	2
Real Resolution [**]	mm	3.3	3.3
Acquisition Time (TA)	min:s	16:44	23:25

[*] The nominal (reconstructed) resolution is the size of the isotropic voxels chosen in the regridding algorithm for reconstructing the images from the 3D radial k-space trajectory.

[**] The real resolution is the resolution calculated from the usual resolution formula: resolution=1/(2×k_{max}), with k_{max} the maximal value of the k-space used for reconstructing the images.

Table 3

Statistics of the intra-subject change in each measure of apparent sodium concentration (ASC) in mM, and the rate of change in each measure of ASC in mM/day, within each cartilage region as determined using each sequence.

		IR Wurst					Radial 3D				
Measure	**Region**	**Mean**	**Std**	**Median**	**IQR**	**P**	**Mean**	**Std**	**Median**	**IQR**	**P**
Change in measure of ASC (mM) [*]											
Mean	LAT	72.73	71.02	48.15	70.63	**0.001**	29.48	44.90	21.70	69.62	**0.034**
Mean	MED	67.53	35.32	61.95	48.35	**0.001**	7.18	30.92	11.10	46.33	0.519
Mean	PAT	73.29	48.81	64.00	40.85	**0.001**	31.42	38.55	34.25	68.48	0.052
Std	LAT	14.82	8.02	13.05	5.33	**0.002**	2.63	8.29	2.00	15.10	0.077
Std	MED	9.58	9.54	5.80	13.60	**0.002**	0.83	7.11	1.00	9.05	0.583
Std	PAT	13.08	12.64	13.10	9.85	**0.001**	3.57	6.66	2.45	8.20	0.391
Rate of change in measure of ASC (mM/day) [**]											
Mean	LAT	0.149	0.084	0.138	0.087	**0.001**	0.064	0.076	0.072	0.146	**0.027**
Mean	MED	0.139	0.065	0.125	0.098	**0.001**	0.014	0.062	0.025	0.098	0.519
Mean	PAT	0.145	0.125	0.105	0.151	**0.001**	0.058	0.086	0.047	0.152	0.052
Std	LAT	0.026	0.022	0.028	0.021	**0.002**	0.007	0.014	0.005	0.018	0.077
Std	MED	0.020	0.020	0.013	0.025	**0.002**	0.002	0.015	0.002	0.017	0.622
Std	PAT	0.030	0.014	0.028	0.012	**0.001**	0.005	0.017	0.004	0.032	0.380

[*] Each P value is calculated from the Wilcoxon test to assess whether the measure changed over time.

[**] Each P value is calculated from the Wilcoxon test to assess whether the rate of change in the measure differed from zero.

Note: P values in bold font represent statistical significance (P<0.05).

Abbreviations: PAT = Patellar cartilage, MED = Femoro-tibial medial cartilage, LAT = Femoro-tibial lateral cartilage, Std = Standard deviation, IQR = Inter-quartile range.